J BONE ONCOL 36 (2022) 100453

Contents lists available at ScienceDirect

Journal of Bone Oncology

journal homepage: www.elsevier.com/locate/jbo

Research Paper

Circular RNA circDOCK1 contributes to osteosarcoma progression by acting as a ceRNA for miR-936 to regulate LEF1

Gang Xu [a], Haijiao Zhang [b], Yuxia Shi [a], Fan Yang [a,*]

[a] Department of Bone and Soft-Tissue Tumor, Shanxi Province Cancer Hospital/ Shanxi Hospital Affiliated to Cancer Hospital, Chinese Academy of Medical Sciences/ Cancer Hospital Affiliated to Shanxi Medical University, Taiyuan, Shanxi, China
[b] The Second Hospital of Shanxi Medical University, Taiyuan, Shanxi, China

HIGHLIGHTS

- CircDOCK1 knockdown relieved osteosarcoma cell malignant behaviors.
- CircDOCK1 functioned as a molecular sponge of miR-936.
- miR-936 directly targeted LEF1.

ARTICLE INFO

Keywords:
CircDOCK1
miR-936
LEF1
Osteosarcoma
Proliferation

ABSTRACT

Background: Osteosarcoma (OS) is a serious bone malignancy that commonly occurred in humans. Recent research suggested that circular RNA (circRNA) Dedicator of cytokinesis 1 (circDOCK1, also called hsa_circ_0020378) enrolled in the tumorigenesis of osteogenic sarcoma. This subject aimed to explore the precise role and mechanism of circDOCK1 on OS progression.

Methods: CircDOCK1, microRNA-936 (miR-936), and Lymphoid enhancer binding factor 1 (LEF1) levels were detected using real-time quantitative polymerase chain reaction (RT-qPCR). Cell Counting Kit-8 (CCK-8), colony formation, 5-ethynyl-2′-deoxyuridine (EdU), transwell, wound healing, and tube formation assays were used to assess OS cell proliferation, migration, invasion, and angiogenesis. Western blot analysis of protein levels of proliferating cell nuclear antigen (PCNA), matrix metalloproteinase 2 (MMP2), MMP9, and LEF1. According to bioinformatics software (circular RNA Interactome and TargetScan) analysis, the binding between miR-936 and circDOCK1 or LEF1 was predicted, followed by verification by a dual-luciferase reporter and RNA Immunoprecipitation (RIP) assays.

Results: Increased circDOCK1 and LEF1, and decreased miR-936 were found in OS tissues and cell lines. Furthermore, circDOCK1 silencing might suppress OS cell proliferation, migration, invasion, and angiogenesis *in vitro*. Bioinformatics analysis exhibited that circDOCK1 acted as a sponge for miR-936 and LEF1 was a downstream target of miR-936. Moreover, circDOCK1 functions through modulation of the miR-936/LEF1 axis.

Conclusion: CircDOCK1 knockdown might attenuate OS cell malignant biological behaviors by regulating the miR-936/GFRA1 axis, which may highlight the diagnostic and therapeutic potential of these molecules for OS treatment.

1. Introduction

As the most prevalent original malignancy in the bone, osteosarcoma (OS), often arises in pediatric sufferers with substantial morbidity [1]. Moreover, it tends to occur in the metaphysis of long bones, accompanied by rapid infiltration and early lung metastasis [2]. Clinically, OS exhibits osteoblastic differentiation and malignant osteoid formation, along with local swelling and pain, limited joint activity, and muscle atrophy [3,4]. In recent years, remarkable advances in the application of combinations of surgical operations with radiotherapy or chemotherapy have acquired favorable outcomes initially [5,6]. However, the survival rate is still quite dismal, which could be attributed to tumor recurrence,

* Corresponding author.
E-mail address: asz6rx@126.com (F. Yang).

https://doi.org/10.1016/j.jbo.2022.100453
Received 23 June 2022; Received in revised form 14 August 2022; Accepted 6 September 2022
Available online 9 September 2022

distant metastasis, and multidrug resistance [7]. Accordingly, there is a need to explore the detailed mechanism of OS to identify a more effective regimen for this tumor treatment.

Currently, some researchers described that a larger part of gene transcripts are actually characterized as non-coding RNAs that play vital regulators in diverse networks, leading to specific cellular responses and fates [8,9]. As a certain class of recently discovered endogenous non-coding RNAs, circRNAs have a highly stable covalent closed continuous loop structure produced by the back splicing events of exons or introns [10,11], which is different from other non-coding RNA. Ubiquitously expressed in eukaryotes, circRNAs might mediate gene expression at various transcriptional levels [12]. Hence, these unique characteristics enable them with potential as biomarkers in human disease diagnosis and prognosis. As a matter of fact, many cellular and animal experiments have confirmed that circRNA dysregulation is enrolled in the modulation of tumor phenotypes [13]. In terms of OS, numerous studies indicated that several circRNAs, such as circ_001422 and circ_001621, were abnormally upregulated in OS and presented a tumor promoter by increasing OS cell proliferation and metastasis [14,15]. Simultaneously, Xu *et al.* found that the circSIPA1L1 absence might attenuate OS cell malignant biological behaviors by regulating the RAB9A signaling pathway [16]. Of note, multiple works of the literature underscored that circDOCK1 (circBase ID: has_circ_0020378) was differentially expressed in a variety of human tumors and partook in initiating tumorigenesis [17,18]. Lately, it has been proved that the upregulation of circDOCK1 might contribute to OS cell carcinogenesis and chemotherapeutic resistance [19]. Nonetheless, its regulatory mechanism in OS progression remains largely unknown.

In the past several years, a large number of experiments exploring the regulatory mechanism of competing endogenous RNAs (ceRNAs) that refer to endogenous RNA transcripts with shared microRNAs (miRNAs) binding sites compete for post-transcriptional control, which has been considered a novel explanation for cancer progression [20,21]. Of note, this mechanism has received increasing attention as the unifying function for circRNAs [22,23]. Herein, our research first discovered that circDOCK1 possesses some binding sites with miR-936 based on the application of the online bioinformatics software. In addition, much literature reported that miR-936 was frequently dysregulated in multiple human cancers and regarded as a tumor-suppressive miRNA by regulating tumor cell malignant biological behaviors [24,25]. Furthermore, it has been confirmed that the overexpression of miR-936 might display anticancer properties by repressing OS cell proliferation, migration, and invasion [26]. Therefore, we further tunneled whether the regulatory role of circDOCK1 on OS development is partly dependent on the miR-936-mediated mechanism.

2. Materials and methods

2.1. Clinical samples and cell culture

Fifty-one fresh OS tissues and paired adjacent non-tumor tissues were provided by the Shanxi Province Cancer Hospital. The detailed clinical characteristics of patients are described in Table 1. Upon resection, tissue samples were instantly snap-frozen in liquid nitrogen and stored at −80℃ until use. None of the subjects received any neoadjuvant therapy, such as radiotherapy or chemotherapy before surgery. Approval to conduct the project was obtained from the Ethics Committee of Shanxi Province Cancer Hospital with written informed consent from all sufferers.

In this study, human OS cell lines: U2OS is p53 and MDM2 normal (CL-0236, Procell, Wuhan, China) and HOS is p53-mutant and CDKN2A (p16)-negative OS (CL-0360, Procell), were cultured in specific mediums (CM-0360, CM-0236, Procell) at 37℃ in 5 % CO_2, respectively. Normal human osteoblast cell line hFOB1.19 (CL-0353, Procell) was routinely incubated in DMEM/F12 with 10 % FBS and 1 % penicillin/streptomycin (Procell) at 34℃.

Table 1
Correlation between circDOCK1 expression and clinicopathological characteristics of OS patients (n = 51).

Clinical feature		circDOCK1		
	N = 51	High (26)	Low (25)	*P* -Value
Age				0.630
≥20	18	10	8	
<20	33	16	17	
Gender				0.461
Male	30	14	16	
Female	21	12	9	
Tumour localisation				0.886
Femur	25	13	12	
Other	26	13	13	
Tumor size				0.065
≥5cm	23	15	8	
<5cm	28	11	17	
Clinical stage				0.017
I + IIA-B	22	7	15	
III	29	19	10	
Distant metastasis				0.018
Yes	24	8	16	
No	27	18	9	

*$P < 0.05$.

2.2. Real-time quantitative polymerase chain reaction (RT-qPCR)

Extraction of total RNAs from tissues and cells was performed using TRIzol reagent (Invitrogen, Paisley Scotland, UK), followed by synthesizing cDNA according to PrimeScript RT Master Mix (Takara, Tokyo, Japan) and All-in-One™ miRNA Fist-Strand cDNA Synthesis Kit (GeneCopoeis, Rockville, MD, USA). After that, an amplification reaction was implemented with an SYBR Green PCR Kit (Takara) on Thermal Cycler CFX6 System (Bio-Rad, Hercules, CA, USA). These target genes were normalized by GAPDH and U6, followed by calculation using the $2^{-\Delta\Delta Ct}$ method. Primer sequences were listed as follows:

circDOCK1: 5′-CCAGAGGCACGTCCAGATTA-3′ (sense), 5′-CAGGAAACTCCGCGTCTAGG-3′ (antisense);

DOCK1: 5′-TATGATGCCAGAGGAGCGGA-3′ (sense), 5′-TGTAACCTCGGTACCACCCT-3′ (antisense);

miR-936: 5′-GCCGAGACAGTAGAGGGAGG-3′ (sense), 5′-CTCAACTGGTGTCGTGGAG-3′ (antisense);

LEF1: 5′-CCCGAAGAGGAAGGCGATTT-3′ (sense), 5′-TCGAGTAGGAGGGTCCCTTG-3′ (antisense);

U6: 5′-CTCGCTTCGGCAGCACA-3′ (sense), 5′-AACGCTTCACGAATTTGCGT-3′ (antisense);

GAPDH: 5′-GACAGTCAGCCGCATCTTCT-3′ (sense), 5′-GCGCCCAATACGACCAAATC −3′ (antisense),

18S rRNA: 5′-AGAAACGGCTACCACATCCA-3′ (sense), 5′-CCCTCCAATGGATCCTCGTT-3′ (antisense).

For the detection of the circDOCK1 distribution, the RNAs derived from cytoplasmic and nuclear extracts were isolated using PARIS Kit (Invitrogen), followed by the assessment of circDOCK1, 18S rRNA (cytoplasm control), and U6 (nucleus control) expression using RT-qPCR. Additionally, to identify the circular feature of this circRNA, total RNAs from OS cell lines were reacted with 4 U/μg of RNase R (Qiagen, Hilden, Germany) for 15 min at 37℃, followed by RT-qPCR analysis.

2.3. Cell transfection

For stable circDOCK1 knockdown, OS cells of 50–80 % confluence were infected with lentiviral vector: short hairpin (sh)-circDOCK1 (sh-circDOCK1#1 and sh-circDOCK1#2) or nontarget control (sh-NC) in media including 6 μg/mL of polybrene, followed by puromycin selection. Meanwhile, 30 nM of the oligonucleotides (RiboBio, Guangzhou, China): miR-936 mimic/inhibitor (miR-936/anti-miR-936) and their controls (NC and anti-NC), and 100 μg of the plasmids (RiboBio):

pcDNA-based circDOCK1 or LEF1 (circDOCK1 or LEF1) and empty pcDNA (circ-NC or vector) were respectively transfected into OS cell lines by means of Lipofectamine 3000 (Invitrogen) for 48 h. Finally, the harvested cells were subject to the assessment of transfection efficiency using RT-qPCR.

2.4. Cell proliferation

To assess OS cell proliferation, Cell Counting Kit-8 (CCK-8), cell colony formation, and 5-ethynyl-2′-deoxyuridine (EdU) assays were conducted. In short, 4000 transfected OS cells were disgested and introduced in 96-well plates, followed by incubation with 10 μL CCK-8 reagent (TransGen Biotech, Beijing, China). 2 h later, the absorbance of the solution was detected under a microplate reader at various time points. For colony formation assay, 500 transfected OS cells were suspended as single cells and introduced into 6-well plates. After being cultured for two weeks to form visible colonies, 4 % formaldehyde (Sigma-Aldrich, St. Louis, MO, USA) was used to fix the colonies, which then were stained with 0.1 % crystal violet (Sigma-Aldrich). At last, the samples of each group were analyzed according to a microscope. For EdU assay, transfected OS cells were reacted with 50 μM EdU (RiboBio) for 2 h. After being mixed with 4 % formaldehyde solution for 30 min, Apollo reaction cocktail and Hoechst were added to each well, followed by visualization using a fluorescence microscope.

2.5. Cell migration and invasion assay

In this assay, the measurement of OS cell migration and invasion was conducted using transwell and wound healing assays. After being resuspended in serum-free medium, the transfected cells were added to the upper chamber with (for invasion assay) without (for migration assay) the Matrigel (BD Biosciences, Heidelberg, Germany). Meanwhile, the medium supplemented with 20 % FBS was loaded into the lower compartment. At 24 h post-incubation, the cells on the lower membrane surfaces were subjected to 0.1 % crystal violet staining (Sigma-Aldrich), followed by the observation using a microscope. For wound healing assay, 1×10^5 transfected OS cells in 6-well plates were cultured overnight to form a monolayer confluence, which then was scratched using a sterile pipette tip. Following removal of the debris, the serum-free medium was introduced into the wells and cultured for 24 h. At length, a microscope and Image J software was applied to capture and assess the wound width of the migrated cells.

2.6. Western blot assay

Using RIPA buffer (Beyotime, Shanghai, China), total protein was extracted from tissues and cells, followed by quantified according to a BCA kit (Sigma-Aldrich). After being separated in the 10 % SDS-PAGE gel, equal amounts of total protein were blotted onto nitrocellulose membranes (Millipore, Molsheim, France), which were orderly probed with primary antibodies: proliferating cell nuclear antigen (PCNA, ab18197, 1:1000, Abcam, Cambridge, MA, USA)), matrix metalloproteinase 2 (MMP2, ab92536, 1:1000, Abcam), MMP9 (ab76003, 1:1000, Abcam), LEF1 (ab137872, 1:1000, Abcam), GAPDH (1:5000, ab181602, Abcam), and the secondary antibody (ab205718, 1:2000, Abcam). Finally, the visualization of blots was performed using the ECL solution (GE Healthcare, Braunschweig, Germany).

2.7. Tube formation assay

In short, serum-starved human umbilical vein endothelial cell HUVECs (Procell) were introduced into 24-well plates coated with Matrigel (BD Biosciences) for 30 min at room temperature to polymerize. After that, the cells at a density of 1×10^4 per well were seeded in wells under a transfected OS cell-conditioned medium. 24 h later, the tube structures formed were imaged under a light microscope.

2.8. Dual-luciferase reporter assay

First of all, the binding sites (between miR-936 and circDOCK1 or LEF1 3′UTR) prediction was conducted using bioinformatics software circular RNA Interactome (https://circinteractome.nia.nih.gov) and TargetScan (https://www.targetscan.org). Then, these sequences were directly synthesized and cloned into psiCHECK-2 vector (Promega, Madison, WI, USA) to generate circDOCK1-wt or LEF1-wt. Meanwhile, their corresponding mutant sequences were also inserted into this vector according to the Site-directed gene mutagenesis kit (Takara), termed circDOCK1-mut or LEF1-mut. After being co-transfected with these constructed vectors and miR-936 or NC into OS cells for 48 h, the luciferase activities in cell lysates were analyzed by a dual-luciferase reporter assay kit (Promega).

2.9. RNA Immunoprecipitation (RIP)

In general, OS cells at 80 %-90 % confluency were lysed in RIP lysis buffer (Millipore). After being divided into two equal parts, the cell lysates were respectively incubated with Ago2 (Millipore) or IgG (Millipore), followed by a mixture with protein A/G magnetic beads at 4℃ overnight. At last, the purified coprecipitated RNA was evaluated using RT-qPCR.

2.10. Tumor xenograft assay

After being approved by the Animal Ethics Committee of the Shanxi Province Cancer Hospital, this animal assay was carried out to validate the impact of circDOCK1 on OS cell growth *in vivo*. Generally, Lentiviral vectors: Lenti-short hairpin (sh)-circDOCK1 for stable circDOCK1 overexpression Lenti-sh-NC were purchased from Geneseed (Guangzhou, China). Then, five weeks old BALB/C nude mice (male, Vital River Laboratory, Beijing, China) were randomly divided into two groups (n = 6 mice per group), followed by subcutaneous injection with 5×10^6 U2OS stably cells transfected with Lenti-sh-circDOCK1 or Lenti-sh-NC. Prior to euthanizing the mice, the measurement of tumor size was performed every 5 days. 30 days later, all mice were euthanatized and the tumor was removed, followed by further analysis. Besides, the excised tumor tissues were fixed in 4 % paraformaldehyde and then paraffin-embedded for Immunohistochemical (IHC) staining, with antibodies specific for Ki67, MMP2, and MMP9 (Abcam).

2.11. Statistical analysis

In this research, all data were analyzed using GraphPad Prism7 (GraphPad Prism software, San Diego, CA, USA) and denoted as mean ± standard deviation (SD). $P < 0.05$ was set as the threshold for statistical significance, which was calculated using Student's *t*-test and one-way analysis of variance (ANOVA) with Tukey's tests.

3. Results

3.1. CircDOCK1 was highly expressed in OS tissues and cells

First of all, circDOCK1 (ID: hsa_circ_0020378) is produced by the back-splicing of exons 6 to 27 of its parental DOCK1 gene, whose spliced mature sequence length is 2848 bp (Fig. 1A). Subsequently, to check the latent roles of circDOCK1 in OS, its expression patterns were detected using RT-qPCR. By contrast with 51 contiguous normal tissues, circDOCK1 content was significantly upregulated in 51 OS tissues (Fig. 1B). To identify the correlation of circDOCK1 expression with clinicopathologic features, the 51 patients with OS were then classified in Table 1. Data exhibited that circDOCK1 expression was associated with tumor size, clinical stage, and distant metastasis ($P < 0.05$). Furthermore, OS cell lines (U2OS and HOS) also exhibited an apparent increase in circDOCK1 expression compared with that in the hFOB 1.19 cells (Fig. 1C).

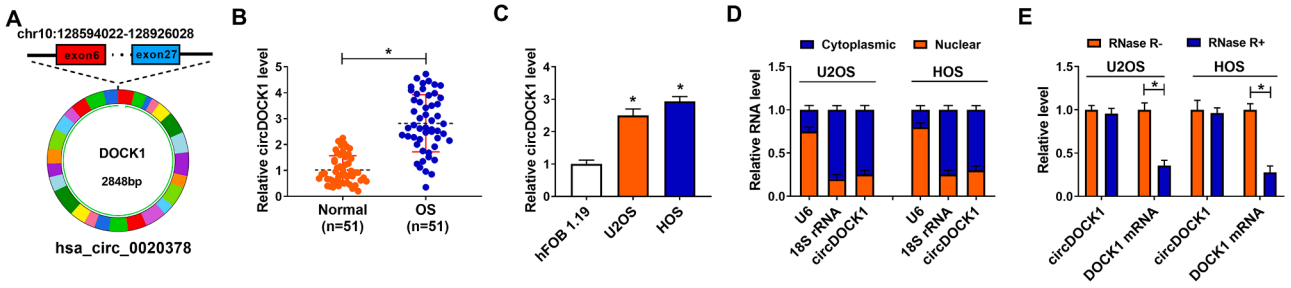

Fig. 1. Expression patterns of circDOCK1 in OS. (A) Schematic illustration suggesting the generation of has_circ_0020378 originated from back-spliced exons 6 to 27 of the DOCK1 gene. (B) RT-qPCR assay was used to assess circDOCK1 expression in 51 pairs of OS tumor tissues and adjacent normal tissues. (C) RT-qPCR analysis of circDOCK1 content in hFOB 1.19 cells, and OS cell lines (U2OS and HOS). (D) The cellular localization of circDOCK1 in OS cell lines was analyzed using Subcellular fractionation assay. (E) RT-qPCR analysis of circDOCK1 and DOCK1 mRNA level in the tumor cells treated with or without RNase R. $^*P < 0.05$.

In addition, the distribution of circDOCK1 was analyzed in the nuclear fraction and the cytoplasmic fraction from these two OS cell lines, and the results discovered that this circRNA was predominantly localized in the cytoplasm (Fig. 1D). After RNase R treatment, our data presented that the levels of the linear forms of DOCK1 sharply reduced, whereas circDOCK1 was resistant to RNase R digestion (Fig. 1E), implying that this circRNA was indeed a circular transcript. Together, these findings suggested that circDOCK1 has a stable circular structure and its

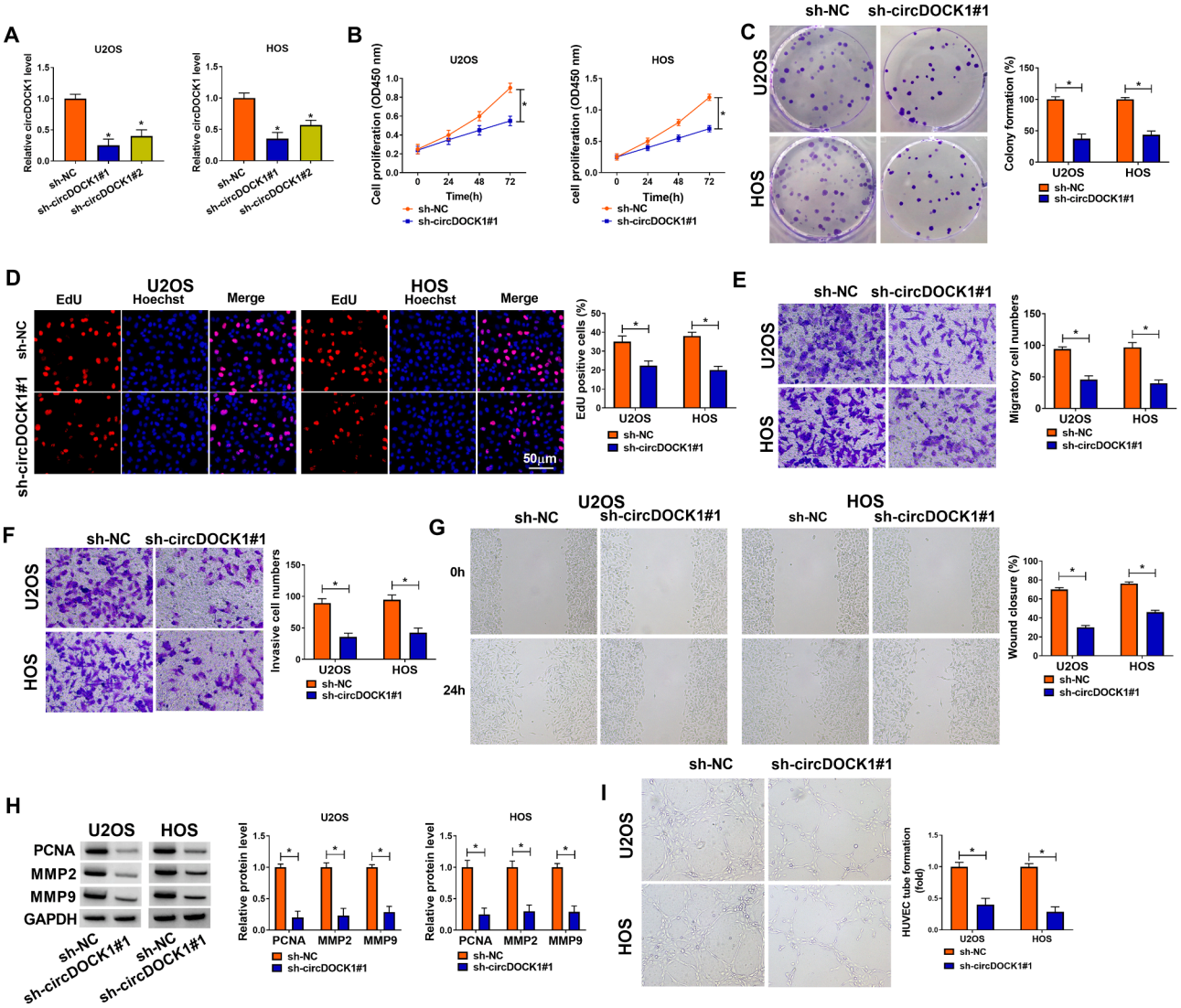

Fig. 2. Downregulation of circDOCK1 might repress cell proliferation, migration, invasion, and angiogenesis of OS cells. (A) The knockdown efficiency of circDOCK1 was detected using RT-qPCR. (B and I) U2OS and HOS cells were transfected with sh-NC or sh-circDOCK1#1. (B-D) OS cell proliferative ability was assessed using CCK-8, colony formation, and EdU assays. (E and F) Transwell analysis of migration and invasion in transfected OS cells. (G) Migration capability was measured using wound heal assay in transfected OS cells. (H) Western blot analysis of PCNA, MMP2, and MMP9 in transfected OS cells. (I) After being treated with the pre-conditioned medium of transfected OS cells, the tube formation of HUVEC was examined using tube formation assay. $^*P < 0.05$.

abnormal expression might be enrolled in the OS process.

3.2. CircDOCK1 deficiency mitigated OS cell malignant biological behaviors

Then, *in vitro* loss-of-function analyses were conducted according to

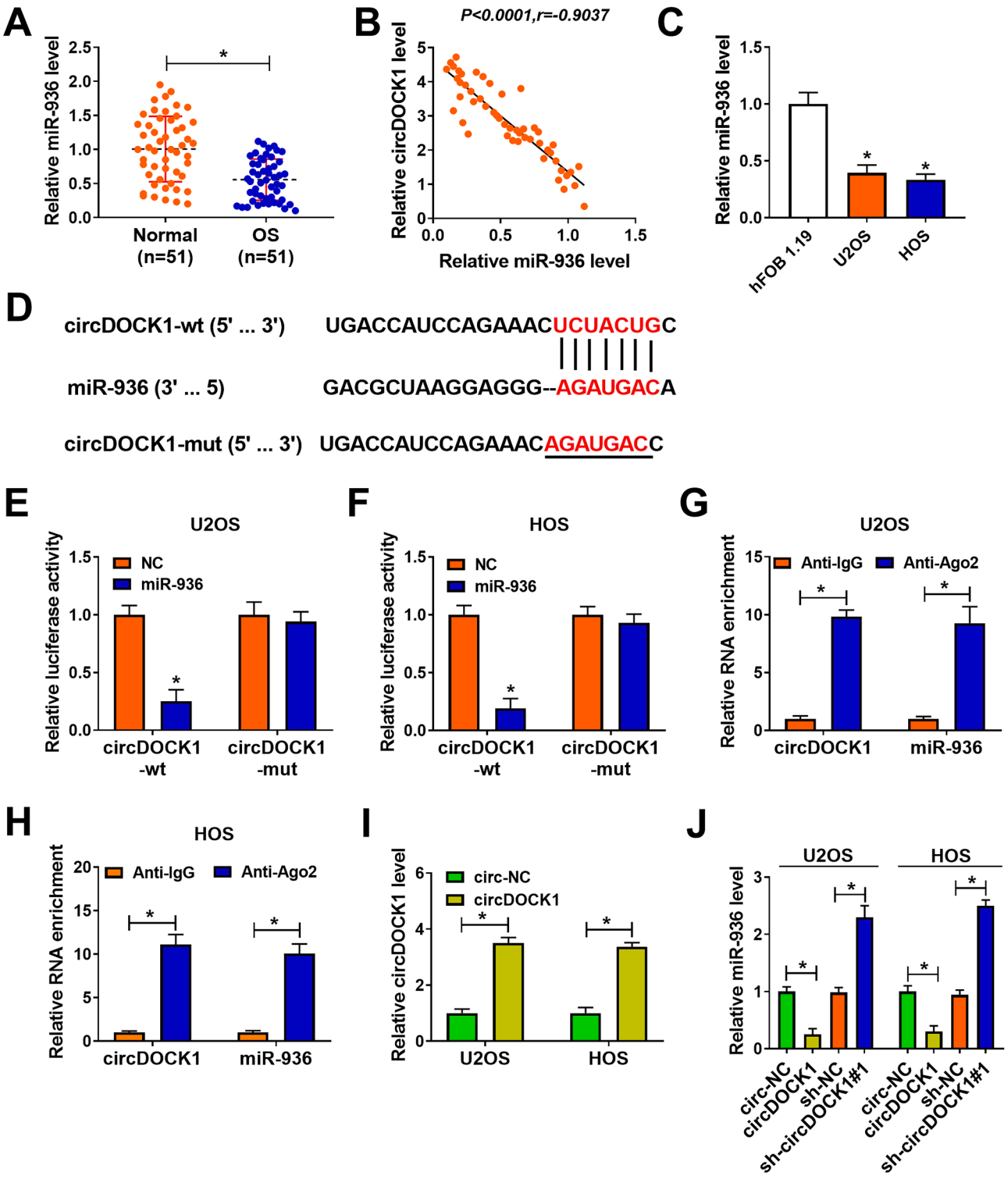

Fig. 3. miR-936 acted as a target of circDOCK1. (A) RT-qPCR analysis of miR-936 expression in OS tumor tissues and adjacent normal tissues. (B) Pearson correlation analysis was used to assess the expression correlation between circDOCK1 and miR-936 in OS tissues. (C) RT-qPCR assay was applied to detect miR-936 content in hFOB 1.19, U2OS, and HOS cells. (D) Schematic of putative target sites for miR-936 in circDOCK1 and mutated miR-936-binding sequence. (E and F) Their binding relationship was verified using a dual-luciferase reporter assay. (G and H) Their interaction was confirmed using RIP assay. (I) The overexpression efficiency of circDOCK1 in OS cells was determined using RT-qPCR assay. (J) RT-qPCR analysis of miR-936 content in U2OS and HOS cells transfected with circ-NC, circDOCK1, sh-NC, and sh-circDOCK1. *$P < 0.05$.

the established circDOCK1 stably knockdown OS cell lines, followed by the measurement of transfection efficiency. As shown in Fig. 2A, the knockdown efficiency of sh-circDOCK1#1 was available since that circDOCK1 expression obviously declined in sh-circDOCK1#1-transfected U2OS and HOS cells relative to both the sh-NC group and the sh-circDOCK1#2 group. After that, CCK-8 assay displayed that the downregulation of circDOCK1 might remarkably dampen U2OS and HOS cell viability (Fig. 2B). In parallel, our data also exhibited that the EdU positive cells and colony number were distinctly dwindled caused by the silencing of circDOCK1 in U2OS and HOS cells (Fig. 2C and 2D). Moreover, transwell assays exhibited an obvious reduction of migration and invasion in U2OS and HOS cells due to circDOCK1 downregulation (Fig. 2E and 2F). Similarly, the result from wound heal assay displayed that migratory capability was markedly hindered by the sh-circDOCK1#1 introduction (Fig. 2G). To identify which proteins in OS cells were modulated through circDOCK1 during cell proliferation, migration, and invasion, western blot assay was performed. As presented in Fig. 2H, PCNA (proliferation marker) and MMP2 and MMP9 (migration/invasion-associated factors) protein levels were significantly decreased via circDOCK1 silencing in U2OS and HOS cells. Beyond that, the tube formation ability of HUVEC cells was strikingly diminished through the treatment with the preconditioned medium of sh-

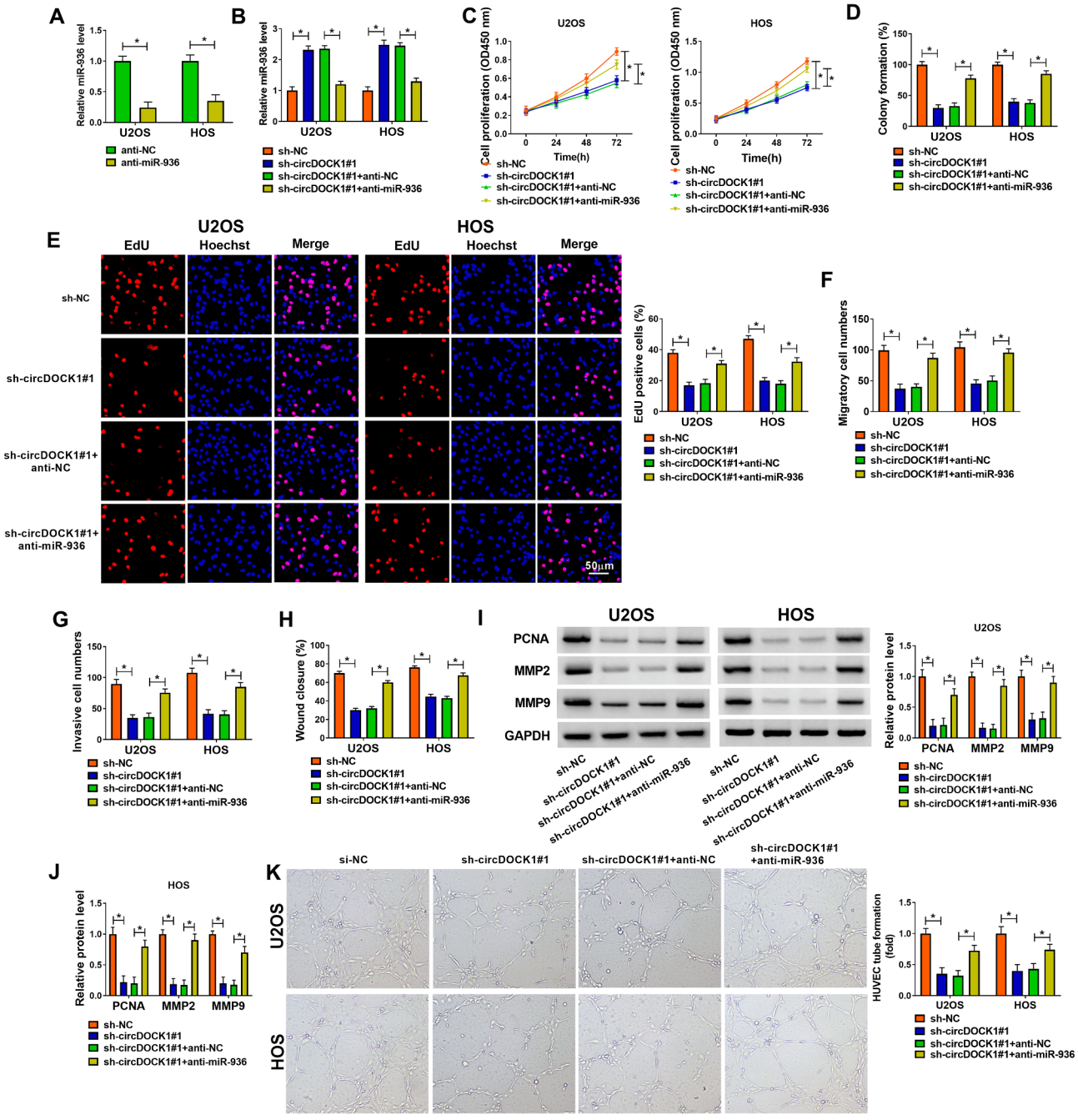

Fig. 4. circDOCK1/miR-936 might regulate OS progression *in vitro*. (A) The knockdown efficiency of miR-936 was assessed using RT-qPCR. (B-K) U2OS and HOS cells were transfected with sh-NC, sh-circDOCK1#1, sh-circDOCK1#1 + anti-NC, and sh-circDOCK1#1 + anti-miR-936. (B) RT-qPCR analysis of miR-936 expression in transfected OS cells. (C-E) CCK-8, colony formation, and EdU assays were performed to measure OS cell proliferative ability. (F-H) Transwell and wound heal assays were conducted to examine OS cell migration and invasion. (I and J) PCNA, MMP2, and MMP9 protein levels were determined using western blot assay in transfected OS cells. (K) Angiogenesis ability was assessed using tube formation assay in transfected OS cells. *$P < 0.05$.

circDOCK1#1 transfected-OS cells (Fig. 2I). Collectively, these results indicated that circDOCK1 knockdown might inhibit the development of OS by decreasing cell proliferation, migration, invasion, and angiogenesis.

3.3. CircDOCK1 served as a miR-936 sponge

A previous study suggested that miR-936 was involved in the regulation of OS progression [26]. Here, RT-qPCR analysis confirmed that miR-936 content was significantly downregulated in OS tumor tissues in comparison with matched normal tissues (Fig. 3A). Of interest, we found that the miR-936 level was negatively associated with the circDOCK1 level in OS tumor tissues (Fig. 3B). Moreover, we further validated an apparent decrease of miR-936 in OS cell lines versus hFOB 1.19 cells (Fig. 3C). Accordingly, Circinteractome software was applied to identify the underlying relationship between miR-936 and circDOCK1, and the results suggested that there were some binding sites between them (Fig. 3D). Then, a dual-luciferase reporter assay exhibited that miR-936 upregulation elicited a significant reduction in luciferase activity of the wild-type group, but had no impact on the mutant-type group (Fig. 3E and 3F). Meanwhile, RIP assay exhibited that both circDOCK1 and miR-936 enrichment was notably increased through anti-AgG2 RIP relative to the IgG control (Fig. 3G and 3H). Additionally, our data presented that circDOCK1 expression was effectively enhanced in circDOCK1-transfected U2OS and HOS cells (Fig. 3I), suggesting a successful transfection efficiency. In U2OS and HOS cells, we noticed that the manipulation of circDOCK1 might alter miR-936 content, presenting as miR-936 decrease with circDOCK1 upregulation and miR-936 increase with circDOCK1 knockdown (Fig. 3J). In all, these results indicated that circDOCK1 might sequester miR-936.

3.4. Knockdown of miR-936 abolished the repression of circDOCK1 silencing on OS cell malignant biological behaviors

Next, rescue experiments were conducted to further verify the influence of circDOCK1 and miR-936 on OS progression. First of all, RT-qPCR analysis discovered that the knockdown efficiency of miR-936 was available because that miR-936 expression was evidently declined in OS cells transfected with anti-miR-936 (Fig. 4A). After that, our data suggested that the introduction of miR-936 inhibitor might partly counteract circDOCK1 absence-triggered increase in miR-936 content in U2OS and HOS cells (Fig. 4B). Functionally, circDOCK1 deficiency was able to significantly block U2OS and HOS cell proliferative ability, while the phenomenon was effectively abrogated by miR-936 downregulation (Fig. 4C-4E). Apart from that, the inhibitory effects of migration and invasion caused by circDOCK1 knockdown were partially reversed via anti-miR-936 con-transfection (Fig. 4F and 4G). Consistently, wound heal analysis indicated that miR-936 downregulation might strikingly overturn circDOCK1 silencing-mediated migratory ability suppression in U2OS and HOS cells (Fig. 4H). In addition, western blot analysis discovered that downregulated circDOCK1 might reduce PCNA, MMP2, and MMP9 protein levels in U2OS and HOS cells, which was notably abolished by miR-936 knockdown (Fig. 4I and 4J), supporting the influences of circDOCK1 and miR-936 on OS cell proliferation, migration, and invasion. Additionally, HUVEC tube formation ability was specially hindered by circDOCK1 deficiency, while the co-transfection of anti-miR-936 might relieve these effects in U2OS and HOS cells (Fig. 4K). Based on the above evidence, circDOCK1 drives OS progression by sponging the tumor suppressor miR-936; miR-936 may be rescued by circDOCK1 knockdown.

3.5. LEF1 worked as a downstream target of miR-936

Furthermore, miRNAs with complementary base matching miR-936 were identified using TargetScan. Here, LEF1 was identified, which had previously been found to be upregulated in various tumors [27], containing OS [28]. Here, RT-qPCR and western blot analysis discovered that LEF1 expression was significantly increased in OS tumor tissues relative to normal tissues (Fig. 5A and 5B). Interestingly, we found that LEF1 content was positively correlated with circDOCK1, while negatively associated with miR-936 in OS tissue samples (Fig. 5C and 5D). Moreover, we further proved an apparent enhancement of LEF1 in OS cell lines relative to hFOB 1.19 cells (Fig. 5E). Simultaneously, the binding sites of LEF1 on miR-936 were depicted in Fig. 5F. Then, a dual-luciferase reporter analysis indicated that miR-936 overexpression might remarkably decrease the luciferase activity of LEF1-wt rather than of LEF1-mut in U2OS and HOS cells (Fig. 5G). Apart from that, the results of RIP assay exhibited that both miR-936 and LEF1 were gathered in Ago2 immunoprecipitates (Fig. 5H). Notably, western blot assay displayed that the co-transfection of anti-miR-936 might effectively counteract sh-circDOCK1#1-induced reduction in LEF1 protein level in U2OS and HOS cells, further supporting the circDOCK1/miR-936/LEF1 axis. Overall, these findings indicate that miR-936 directly interacted with LEF1 in OS cells.

3.6. miR-936/LEF1 regulated the OS cell malignant behaviors in vitro

To further explore the cross-talk between miR-936 and LEF1 on OS progression, we performed rescue assays in U2OS and HOS cells. At first, the overexpression efficiency of miR-936 or LEF1 was available, considering that their levels were significantly upregulated in miR-936 or LEF1-transfected OS cell lines compared with control groups (Fig. 6A and 6B). After that, the results of western blot assay presented that the upregulation of miR-936 was able to dwindle LEF1 content in these two OS cell lines, which was significantly counteracted after LEF1 co-transfection (Fig. 6C). Functional analysis suggested that the LEF1 overexpression might largely abolish the suppressive effect of miR-936 mimic on cell proliferative ability in OS cells (Fig. 6D-6F), as evidenced by increased PCNA (Fig. 6J). Beyond that, transwell and wound healing assays indicated that miR-936 overexpression-mediated migration and invasion repression was partly reversed through LEF1 upregulation in OS cells (Fig. 6G-6I), accompanied by higher MMP2 and MMP9 (Fig. 6J). In addition, tube formation assay displayed that enhanced LEF1 might remarkably attenuate the negative action of miR-936 overexpression on OS cell angiogenesis ability (Fig. 6K). Namely, we concluded that miR-936 might relieve OS cell malignant behaviors by targeting LEF1.

3.7. Downregulation of circDOCK1 inhibited the growth of xenograft tumors in vivo

In addition, to confirm the functional effects of circDOCK1 on tumor growth *in vivo*, a xenograft tumor mouse model was established. In the *in vivo* experiments, we found that the tumors derived from the circDOCK1-deficient cells were much smaller than the control tumors (Fig. 7A and 7B). Beyond that, in the removed tumor tissues, the expression of circDOCK1, LEF1, and PCNA in the sh-circDOCK1 group was prominently diminished versus the sh-NC group, while miR-936 level displayed the opposite effects (Fig. 7C and 7D). Additionally, upon staining the tumor sections to assess ki67 (a proliferation marker), MMP2, and MMP9 expression, data discovered that the ki67, MMP2, and MMP9 content was strikingly diminished in the sh-circDOCK1 group compared with the sh-NC group (Fig. 7E). Together, these results indicated that circDOCK1 silencing might hinder the tumor growth of OS *in vivo*.

4. Discussion

For more than 30 years, the existence of circRNAs with covalently closed circular structures was sporadically reported and once counted as erroneous splicing products or by-products of mRNA splicing [29]. In recent years, advances in bioinformatics prediction coupled with RNA

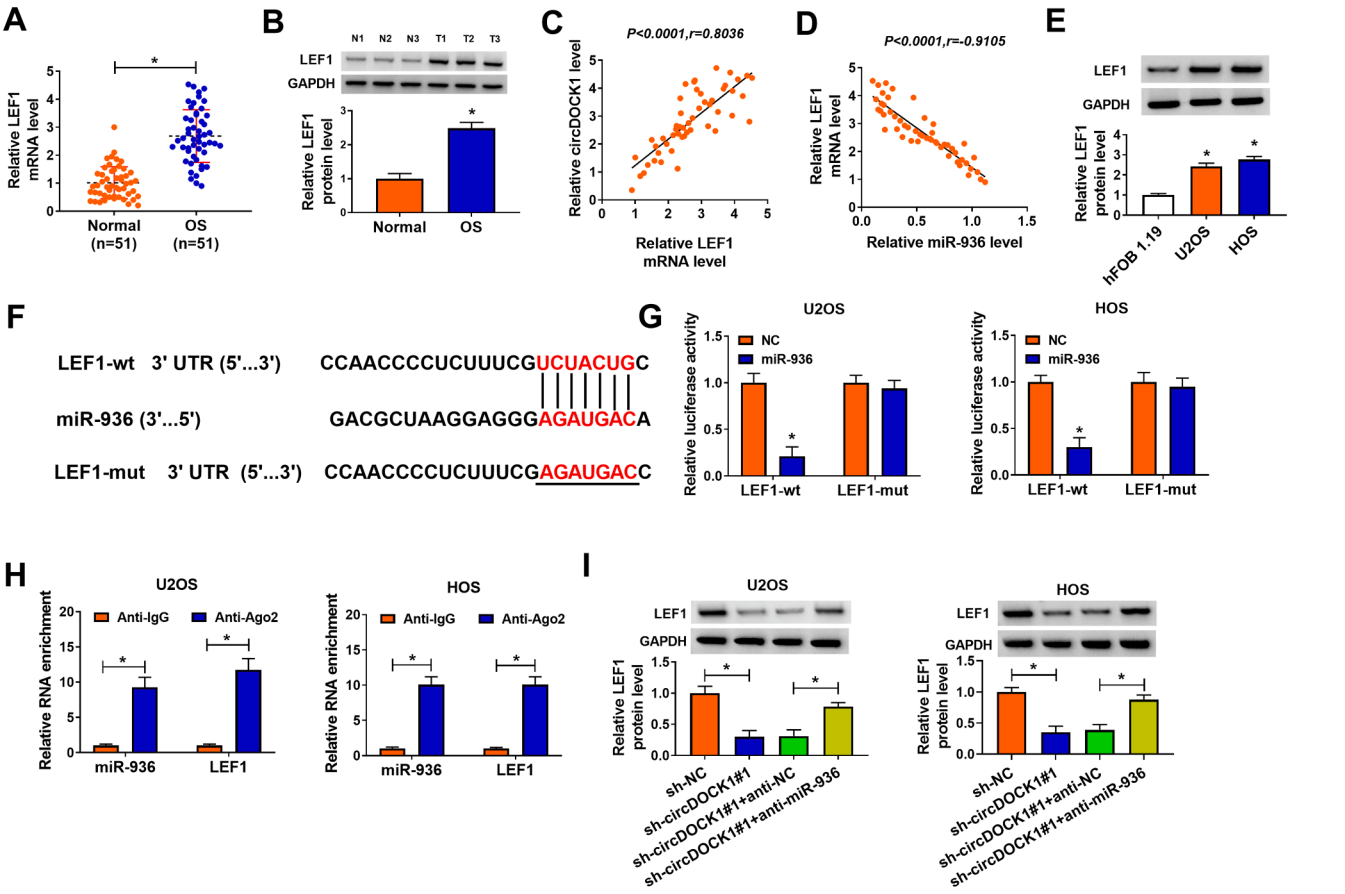

Fig. 5. miR-936 directly targeted LEF1. (A and B) RT-qPCR and western blot analysis of LEF1 expression in OS tumor tissues and normal tissues. (C and D) Expression association of LEF1 with miR-936 and circDOCK1 in OS tumor tissues was analyzed according to Pearson correlation analysis. (E) LEF1 protein level was determined in hFOB 1.19, U2OS, and HOS cells using western blot assay. (F) TargetScan was used to predicate the binding sequence between miR-936 and LEF13′UTR. (G and H) Their binding relationship was verified using a dual-luciferase reporter and RIP assays. (I) Western blot analysis of LEF1 protein level in U2OS and HOS cells transfected with sh-NC, sh-circDOCK1#1, sh-circDOCK1#1 + anti-NC, and sh-circDOCK1#1 + anti-miR-936. $^*P < 0.05$.

sequencing technologies application have prominently improved the knowledge of circRNAs [30,31]. Recent studies have indicated that numerous of circRNAs were highly stable and abundantly expressed functional RNA molecules, which exhibited diverse fundamental biological activities [32]. Compared with other types of non-coding RNAs, circRNAs have emerged as more reliable and promising disease biomarkers [33]. In fact, much laboratory work has highlighted the importance of circRNA dysregulation in some human malignant tumors [34]. At present, it has become evident that the number of OS-associated circRNAs with verified biological functions and mechanisms of action is growing [35]. Here, our work identified a typical exonic circRNA with a circular structure, circDOCK1, which is derived from the parental gene DOCK1. Coincided with the former report [19], circDOCK1 content was freakishly upregulated in OS tissues and cell lines. Apart from that, *in vitro* loss-of-function experiments delineated that circDOCK1 absence might dampen cell proliferation, migration, and invasion of OS cells *in vitro*. In addition, it has been confirmed that angiogenesis is a process of vascular remodeling, which is critical for development and tissue growth. However, pathological angiogenesis is a multistep process that can lead to aberrantly formed and organized vessels with enhanced permeability and boost tumor growth and metastases, which was recognized as one of the hallmarks of most solid tumors [36], including OS [37]. Beyond that, there has been any amount of research presenting that circRNAs have a strong ability to modulate angiogenesis recently [38]. Subsequently, we further explored the influences of circDOCK1 on angiogenesis in OS. As expected, the current work proved the inhibitory action of circDOCK1 silencing on angiogenesis in OS cells. In parallel, our data also validated the repression effect of circDOCK1 downregulation on OS cell growth *in vivo*. From the above findings, it is delineated that the oncogenic role of circDOCK1 on OS development, which provide a strong basis for this tumor clinical practice.

Nowadays, the regulatory network of circRNA-miRNA-mRNA has caught more and more attention in human tumor research [21]. Researchers described that most circRNAs have miRNA-binding sites that might function as miRNA sponges to alter their target gene expression [23,39]. Furthermore, it has been verified that the cellular sublocalization of circRNAs is required for this regulatory mechanism [40]. In this research, circDOCK1 expression was checked to be mainly distributed in the cytoplasmic OS cells. After the application of the circular RNA Interactome tool, the present work proposed that circDOCK1 might act as ceRNA for miR-936, followed by verifying the dual-luciferase reporter and RIP analysis. Apart from that, some studies have indicated that miR-936 is often abnormally reduced in various human tumors and participated in inhibiting the malignant behavior of tumor cells [41,42]. Moreover, relevant studies validated the suppressive role of miR-936 on OS cell growth and metastasis [26]. In this work, our results indicated that miR-936 content was significantly decreased in OS, and its knockdown was able to abolish circDOCK1 downregulation-mediated OS cell proliferation, invasion, migration, and angiogenesis inhibition. Of note, much of the current literature manifested that circDOCK1 might impede the proliferation and migration potential in OS cells, thyroid cancer cells, and bladder carcinoma cells by sponging different miRNAs [17,18]. Accordingly, we infer that circDOCK1, acting as a sponge of multiple miRNAs, partake in a more

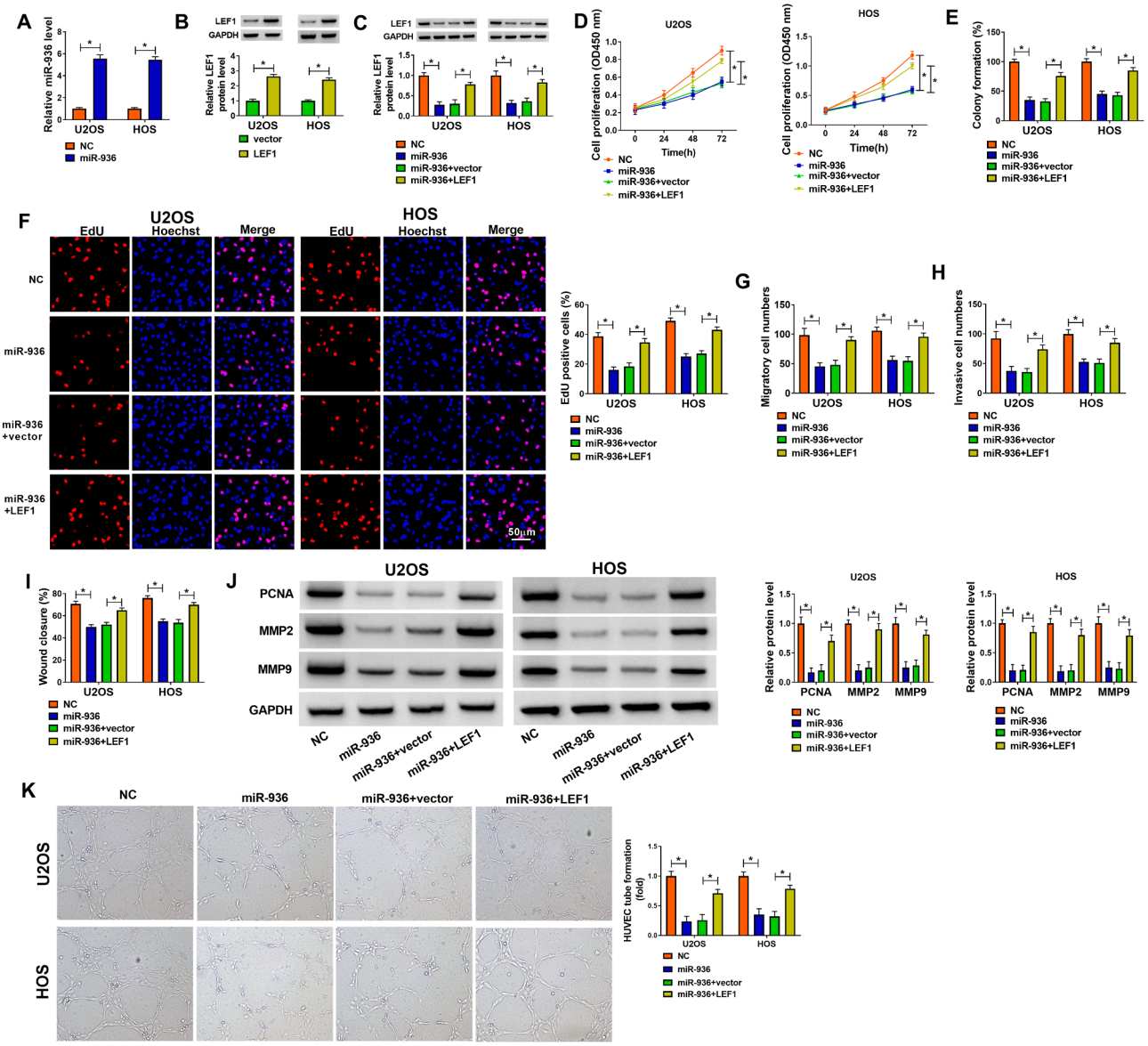

Fig. 6. LEF1 overexpression ameliorated the influence of miR-936 on OS cell malignant behaviors. (A) RT-qPCR analysis was used to assess the transfection efficiency of miR-936 mimic in U2OS and HOS cells. (B) Western blot assay was applied to detect the overexpression efficiency of LEF1 in these two OS cell lines. (C-K) U2OS and HOS cells were transfected with NC, miR-936, miR-936 + vector, and miR-936 + LEF1. (C) Western blot analysis of LEF1 content in transfected OS cells. (D-F) The assessment of OS cell proliferative ability was conducted using CCK-8, colony formation, and EdU assays. (G-I) The measurement of migration and invasion was performed using Transwell and wound heal assays. (J) The detection of PCNA, MMP2, and MMP9 protein levels was implemented using western blot assay. (K) The analysis of angiogenesis ability was executed using tube formation assay in transfected OS cells. $^{*}P < 0.05$.

comprehensive circRNAs-miRNAs co-expression network during cancer development, containing OS.

LEF1 is a transcription factor located on chromosome 4q25, which belongs to a homologous family with high mobility groups protein and nuclear effector of the canonical Wnt signaling pathway [27]. Moreover, it has been confirmed that this pathway might influence bond density via regulating postnatal osteoblast proliferation [43]. Meanwhile, LEF1 was reported to take part in the regulation of osteogenic differentiation via the β-catenin pathway [44]. In this paper, our data suggested that LEF1 content was obviously increased in OS tissues and cells, consistent with the earlier report [45]. In line with the analysis of TargetScan software, LEF1 appeared as a probable target of miR-936, as proved by a dual-luciferase reporter and RIP assay. Subsequently, the functional analysis indicated that miR-936 might relieve OS cell malignant biological behaviors through interacting with LEF1. Importantly, western blot analysis displayed that circDOCK1 deficiency might restrain LEF1 content in OS cells, and these influences were effectively counteracted via miR-936 downregulation, which further supports the ceRNA regulatory network of circDOCK1/miR-936/LEF1 in OS in this research. Interestingly, a previous report suggested that MMP9 is a key driver of OS metastasis [46]. In this work, our data exhibited that the inhibitory role of circDOCK1 silencing on the MMP9 protein level was regulated by the miR-936/LEF1 axis in OS cell lines, further verifying the regulatory role of the ceRNA regulatory network on OS metastasis. Frankly speaking, this project has still some shortcomings. For instance, more clinical samples from the different regions were needed to be used to verify our findings, considering the limited sample size.

5. Conclusion

In summary, these results uncovered that circDOCK1 absence might attenuate OS cell malignant behaviors by targeting the miR-936/LEF1

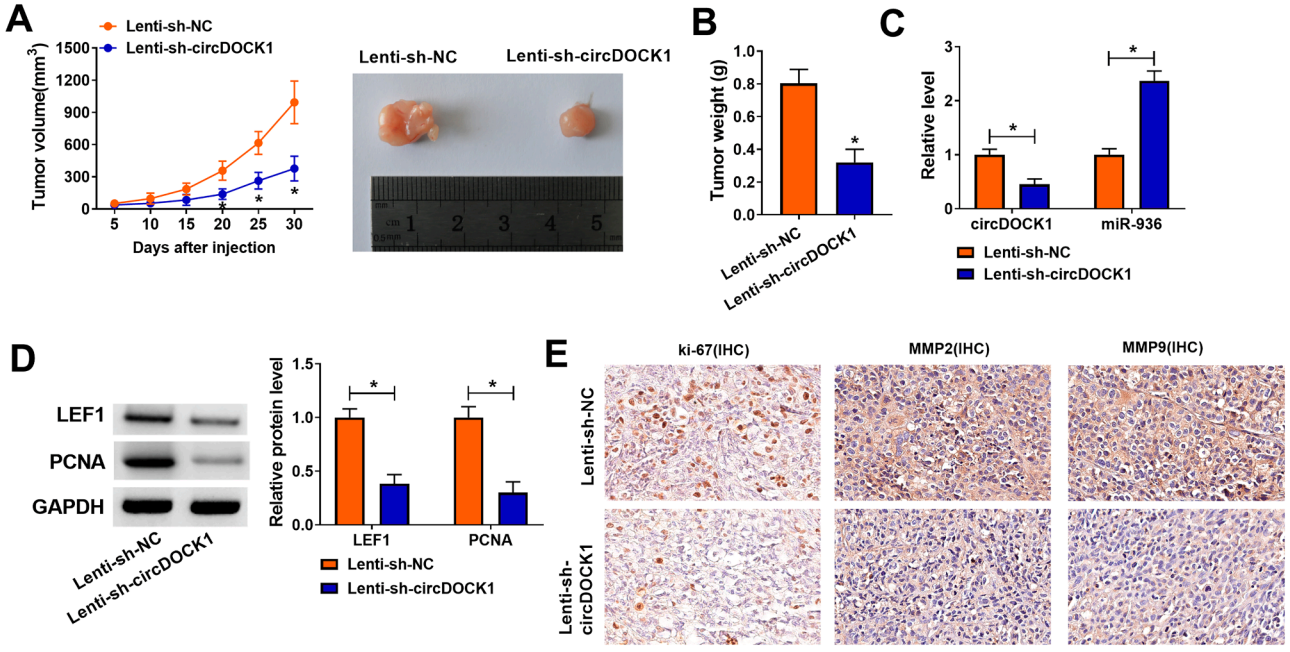

Fig. 7. The depletion of circDOCK1 restrained OS cell growth *in vivo*. Nude mice were subcutaneously injected with HOS cells stably transfected with sh-circDOCK1 or sh-NC. (A) Growth curve of xenografted tumors. (B) The assessment of tumor weight was carried out. (C and D) Expression of circDOCK1, miR-936, LEF1, and PCNA was determined in the obtained mice tumor tissues using RT-qPCR and western blot assays. (E) IHC staining analysis of ki67, MMP2, and MMP9 expression in these mice tumor tissues. $^*P < 0.05$.

axis, providing an available preclinical basis for this tumor.

6. Declarations

Ethics approval and consent to participate

The present study was approved by the ethical review committee of Shanxi Province Cancer Hospital. Written informed consent was obtained from all enrolled patients.

Consent for publication

Patients agree to participate in this work

Availability of data and materials

The analyzed data sets generated during the present study are available from the corresponding author on reasonable request.

Funding

This work was supported by Shanxi applied basic research program (Grant No.NO.201901D111371).

CRediT authorship contribution statement

Gang Xu: Validation, Investigation, Writing – original draft, Writing – review & editing. **Haijiao Zhang:** Software, Validation, Investigation, Conceptualization, Methodology, Writing – original draft, Writing – review & editing. **Yuxia Shi:** Formal analysis, Data curation, Conceptualization, Methodology, Writing – original draft, Writing – review & editing. **Fan Yang:** Project administration, Formal analysis, Data curation, Writing – original draft, Writing – review & editing.

Declaration of Competing Interest

The authors declare that they have no known competing financial interests or personal relationships that could have appeared to influence the work reported in this paper.

Acknowledgement

Not applicable

References

[1] D.D. Moore, H.H. Luu, Osteosarcoma, Cancer Treat Res. 162 (2014) 65–92.
[2] I. Yaman Bajin, N. Kurucu, B. Oguz, Z. Akcoren, A. Varan, O. Satirer, C. Akyuz, Primary osteosarcoma of the rib: A case report and review of the literature, J Pediatr Hematol Oncol. 40 (2018) 48–50.
[3] T. Quist, H. Jin, J.-F. Zhu, K. Smith-Fry, M.R. Capecchi, K.B. Jones, The impact of osteoblastic differentiation on osteosarcomagenesis in the mouse, Oncogene 34 (32) (2015) 4278–4284.
[4] H. Nouri, M. Ben Maitigue, L. Abid, N. Nouri, A. Abdelkader, M. Bouaziz, M. Mestiri, Surface osteosarcoma: Clinical features and therapeutic implications, J Bone Oncol. 4 (2015) 115–123.
[5] A. Luetke, P.A. Meyers, I. Lewis, H. Juergens, Osteosarcoma treatment - where do we stand? A state of the art review, Cancer Treat Rev. 40 (4) (2014) 523–532.
[6] R. Belayneh, M.S. Fourman, S. Bhogal, K.R. Weiss, Update on osteosarcoma, Curr Oncol Rep. 23 (2021) 71.
[7] M.E. Anderson, Update on survival in osteosarcoma, Orthop Clin North Am. 47 (1) (2016) 283–292.
[8] S. Panni, R.C. Lovering, P. Porras, S. Orchard, Non-coding RNA regulatory networks, Biochim. Biophys. Acta Gene Regul. Mech. 1863 (2020).
[9] P.E. Saw, X. Xu, J. Chen, E.-W. Song, Non-coding RNAs: the new central dogma of cancer biology, Sci China Life Sci. 64 (1) (2021) 22–50.
[10] I.L. Patop, S. Wust, S. Kadener, Past, present, and future of circRNAs, EMBO J. 38 (2019) e100836.
[11] S.P. Barrett, P.L. Wang, J. Salzman, Circular RNA biogenesis can proceed through an exon-containing lariat precursor, Elife. 4 (2015) e07540.
[12] S. Memczak, M. Jens, A. Elefsinioti, F. Torti, J. Krueger, A. Rybak, L. Maier, S. D. Mackowiak, L.H. Gregersen, M. Munschauer, A. Loewer, U. Ziebold, M. Landthaler, C. Kocks, F. le Noble, N. Rajewsky, Circular RNAs are a large class of animal RNAs with regulatory potency, Nature 495 (7441) (2013) 333–338.
[13] I.L. Patop, S. Kadener, circRNAs in Cancer, Curr Opin Genet Dev. 48 (2018) 121–127.
[14] B. Yang, L. Li, G. Tong, Z. Zeng, J. Tan, Z. Su, Z. Liu, J. Lin, W. Gao, J. Chen, S. Zeng, G. Wu, L. Li, S. Zhu, Q. Liu, L. Lin, Circular RNA circ_001422 promotes the progression and metastasis of osteosarcoma via the miR-195-5p/FGF2/PI3K/Akt axis, J. Exp. Clin. Cancer Res. 40 (2021) 235.
[15] X. Ji, L. Shan, P. Shen, M. He, Circular RNA circ_001621 promotes osteosarcoma cells proliferation and migration by sponging miR-578 and regulating VEGF expression, Cell Death Dis. 11 (2020) 18.
[16] Y. Xu, T. Yao, H. Ni, R. Zheng, K. Huang, Y. Huang, J. Gao, D. Qiao, S. Shen, J. Ma, Circular RNA circSIPA1L1 contributes to osteosarcoma progression through the miR-411-5p/RAB9A signaling pathway, Front. Cell Dev. Biol. 9 (2021) 642605.

[17] P. Liu, X. Li, X. Guo, J. Chen, C. Li, M. Chen, L. Liu, X. Zhang, X. Zu, Circular RNA DOCK1 promotes bladder carcinoma progression via modulating circDOCK1/hsa-miR-132-3p/Sox5 signalling pathway, Cell Prolif. 52 (2019) e12614.
[18] W. Cui, J. Xue, Circular RNA DOCK1 downregulates microRNA-124 to induce the growth of human thyroid cancer cell lines, BioFactors 46 (2020) 591–599.
[19] S. Li, F. Liu, K. Zheng, W. Wang, E. Qiu, Y. Pei, S. Wang, J. Zhang, X. Zhang, CircDOCK1 promotes the tumorigenesis and cisplatin resistance of osteogenic sarcoma via the miR-339-3p/IGF1R axis, Mol Cancer. 20 (2021) 161.
[20] A. Sanchez-Mejias, Y. Tay, Competing endogenous RNA networks: tying the essential knots for cancer biology and therapeutics, J. Hematol. Oncol. 8 (2015) 30.
[21] X. Qi, D.H. Zhang, N. Wu, J.H. Xiao, X. Wang, W. Ma, ceRNA in cancer: possible functions and clinical implications, J. Med. Genet. 52 (2015) 710–718.
[22] Y. Zhong, Y. Du, X. Yang, Y. Mo, C. Fan, F. Xiong, D. Ren, X. Ye, C. Li, Y. Wang, F. Wei, C. Guo, X. Wu, X. Li, Y. Li, G. Li, Z. Zeng, W. Xiong, Circular RNAs function as ceRNAs to regulate and control human cancer progression, Mol. Cancer. 17 (2018) 79.
[23] A.C. Panda, Circular RNAs Act as miRNA Sponges, Adv. Exp. Med. Biol. 1087 (2018) 67–79.
[24] L. Xu, W. Li, Q. Shi, M. Wang, H. Li, X. Yang, J. Zhang, MicroRNA936 inhibits the malignant phenotype of retinoblastoma by directly targeting HDAC9 and deactivating the PI3K/AKT pathway, Oncol. Rep. 43 (2020) 635–645.
[25] S. Liu, Y. Gong, X.D. Xu, H. Shen, S. Gao, H.D. Bao, S.B. Guo, X.F. Yu, J. Gong, MicroRNA-936/ERBB4/Akt axis exhibits anticancer properties of gastric cancer through inhibition of cell proliferation, migration, and invasion, Kaohsiung J. Med. Sci. 37 (2021) 111–120.
[26] S. Ding, G. Zhang, Y. Gao, S. Chen, C. Cao, Circular RNA hsa_circ_0005909 modulates osteosarcoma progression via the miR-936/HMGB1 axis, Cancer Cell Int. 20 (2020) 305.
[27] L. Santiago, G. Daniels, D. Wang, F.M. Deng, P. Lee, Wnt signaling pathway protein LEF1 in cancer, as a biomarker for prognosis and a target for treatment, Am. J. Cancer Res. 7 (2017) 1389–1406.
[28] W. Miao, J. Chen, L. Jia, J. Ma, D. Song, The m6A methyltransferase METTL3 promotes osteosarcoma progression by regulating the m6A level of LEF1, Biochem. Biophys. Res. Commun. 516 (3) (2019) 719–725.
[29] C. Cocquerelle, B. Mascrez, D. Hétuin, B. Bailleul, Mis-splicing yields circular RNA molecules, FASEB J. 7 (1) (1993) 155–160.
[30] E. Lopez-Jimenez, A.M. Rojas, E. Andres-Leon, RNA sequencing and Prediction Tools for Circular RNAs Analysis, Adv. Exp. Med. Biol. 1087 (2018) 17–33.
[31] G. Ferrero, N. Licheri, M. De Bortoli, R.A. Calogero, M. Beccuti, F. Cordero, Computational Analysis of circRNA Expression Data, Methods Mol. Biol. 2284 (2021) 181–192.
[32] R.A. Wesselhoeft, P.S. Kowalski, D.G. Anderson, Engineering circular RNA for potent and stable translation in eukaryotic cells, Nat. Commun. 9 (2018) 2629.
[33] B. Lei, Z. Tian, W. Fan, B. Ni, Circular RNA: a novel biomarker and therapeutic target for human cancers, Int J Med Sci. 16 (2019) 292–301.
[34] L.S. Kristensen, T.B. Hansen, M.T. Veno, J. Kjems, Circular RNAs in cancer: opportunities and challenges in the field, Oncogene 37 (2018) 555–565.
[35] Z. Li, X. Li, D. Xu, X. Chen, S. Li, L. Zhang, M.T.V. Chan, W.K.K. Wu, An update on the roles of circular RNAs in osteosarcoma, Cell Prolif. 54 (2021) e12936.
[36] C. Viallard, B. Larrivee, Tumor angiogenesis and vascular normalization: alternative therapeutic targets, Angiogenesis 20 (2017) 409–426.
[37] Y. Liu, N. Huang, S. Liao, E. Rothzerg, F. Yao, Y. Li, D. Wood, J. Xu, Current research progress in targeted anti-angiogenesis therapy for osteosarcoma, Cell Prolif. 54 (2021) e13102.
[38] Y. Liu, Y. Yang, Z. Wang, X. Fu, X.M. Chu, Y. Li, Q. Wang, X. He, M. Li, K. Wang, J. X. Wang, P.F. Li, T. Yu, Insights into the regulatory role of circRNA in angiogenesis and clinical implications, Atherosclerosis. 298 (2020) 14–26.
[39] T.B. Hansen, T.I. Jensen, B.H. Clausen, J.B. Bramsen, B. Finsen, C.K. Damgaard, J. Kjems, Natural RNA circles function as efficient microRNA sponges, Nature 495 (7441) (2013) 384–388.
[40] L.-L. Chen, The biogenesis and emerging roles of circular RNAs, Nat Rev Mol Cell Biol. 17 (4) (2016) 205–211.
[41] X.J. Lin, H. Liu, P. Li, H.F. Wang, A.K. Yang, J.M. Di, Q.W. Jiang, Y. Yang, J. R. Huang, M.L. Yuan, Z.H. Xing, M.N. Wei, Y. Li, Z. Shi, J. Ye, miR-936 Suppresses Cell Proliferation, Invasion, and Drug Resistance of Laryngeal Squamous Cell Carcinoma and Targets GPR78, Front Oncol. 10 (2020) 60.
[42] D. Zhou, X. Lin, P. Wang, Y. Yang, J. Zheng, D. Zhou, Circular RNA circ_0001162 promotes cell proliferation and invasion of glioma via the miR-936/ERBB4 axis, Bioengineered. 12 (1) (2021) 2106–2118.
[43] R.T. Moon, B. Bowerman, M. Boutros, N. Perrimon, The promise and perils of Wnt signaling through beta-catenin, Science 296 (2002) 1644–1646.
[44] Y. Luo, R. Ge, H. Wu, X. Ding, H. Song, H. Ji, M. Li, Y. Ma, S. Li, C. Wang, H. Du, The osteogenic differentiation of human adipose-derived stem cells is regulated through the let-7i-3p/LEF1/beta-catenin axis under cyclic strain, Stem Cell Res Ther. 10 (2019) 339.
[45] G. Qin, X. Wu, Circular RNA hsa_circ_0032463 Acts as the Tumor Promoter in Osteosarcoma by Regulating the MicroRNA 498/LEF1 Axis, Mol Cell Biol. 41 (2021) e0010021.
[46] D. Green, H. Eyre, A. Singh, J.T. Taylor, J. Chu, L. Jeys, V. Sumathi, A. Coonar, D. Rassl, M. Babur, D. Forster, S. Alzabin, F. Ponthan, A. McMahon, B. Bigger, T. Reekie, M. Kassiou, K. Williams, T. Dalmay, W.D. Fraser, K.G. Finegan, Targeting the MAPK7/MMP9 axis for metastasis in primary bone cancer, Oncogene 39 (33) (2020) 5553–5569.